JACS
JOURNAL OF THE AMERICAN CHEMICAL SOCIETY
Article
pubs.acs.org/JACS

Zn_2NF and Related Analogues of ZnO

Srinivasa Rao Lingampalli,[†] Krishnappa Manjunath,[†] Sandhya Shenoy,[‡] Umesh V. Waghmare,[‡] and C. N. R. Rao*[,†]

[†]New Chemistry Unit, International Centre for Materials Science, CSIR Centre of Excellence in Chemistry, Sheikh Saqr Laboratory, Jawaharlal Nehru Centre for Advanced Scientific Research, Jakkur, Bangalore-560064, India

[‡]Theoretical Sciences Unit, Jawaharlal Nehru Centre for Advanced Scientific Research, Jakkur, Bangalore-560064, India

Supporting Information

ABSTRACT: Substitution of aliovalent N^{3-} and F^- anions in place of O^{2-} in ZnO brings about major changes in the electronic structure and properties, the composition, even with 10 atomic percent or less of the two anions, rendering the material yellow colored with a much smaller band gap. We have examined the variation of band gap of ZnO with progressive substitution of N and F and more importantly prepared Zn_2NF which is the composition one obtains ultimately upon complete replacement of O^{2-} ions. In this article, we present the results of a first complete study of the crystal and electronic structures as well as of properties of a stable metal nitride fluoride, Zn_2NF. This material occurs in two crystal forms, tetragonal and orthorhombic, both with a band gap much smaller than that of ZnO. Electronic structures of Zn_2NF as well as $ZnO_{0.2}N_{0.5}F_{0.3}$ investigated by first-principles calculations show that the valence bands of these are dominated by the N (2p) states lying at the top. Interestingly, the latter is a p-type material, a property that has been anticipated for long time. The calculations predict conduction and valence band edges in Zn_2NF to be favorable for water splitting. Zn_2NF does indeed exhibit good visible-light-induced hydrogen evolution activity unlike ZnO. The present study demonstrates how aliovalent anion substitution can be employed for tuning band gaps of materials.

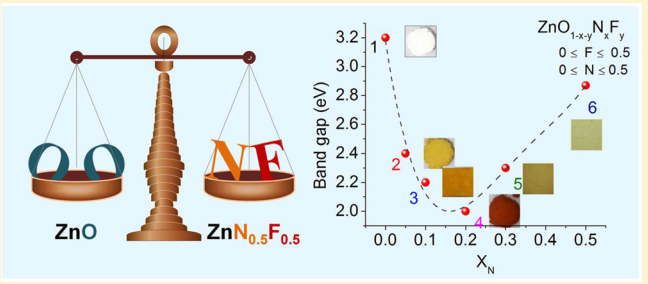

1. INTRODUCTION

It has been shown recently that substitution of aliovalent anions in inorganic materials gives rise to remarkable consequences unlike substitution of isovalent anions.[1,2] The band gap of a material depends on the extent of the overlap of the valence orbitals and the electronegativity difference between the cation and anion. Increase in the spatial overlap between their orbitals of and electronegativity difference results in an increase in the band gap.[3] Band gap modification in several materials has been accomplished by adopting these ideas.[4,5] Thus, oxynitrides of perovskites have been modified to tune the optical absorption for use as inorganic pigments and photocatalytsts for water splitting.[4,6] Substitution of N^{3-} and F^- in an oxide brings about major changes in the electronic structure and properties, thereby providing a means of tuning band gaps in materials.[7,8]

In the present context, we are concerned with the change in the band gap with the substitution of N^{3-} and F^- in ZnO, wherein the material becomes colored and allows visible light excitation.[7,9,10] Substitution of sulfide anions in place of the oxide anion does not have such significant effects.[11] The purpose of substituting both N^{3-} an F^- is to eliminate or minimize anion vacancies which would form with the substitution of N^{3-} alone.[7,12] If one were to substitute the oxide ions in ZnO progressively with N and F, one would ultimately obtain Zn_2NF. We have investigated the crystal and electronic structure as well as important properties of Zn_2NF, which is a stable compound. There are a few reports in the literature[8,13−15] on metal nitride fluorides mainly of the type A_2NF (A = alkaline earth) based on the suggestions of Andersson[16,17] that two O^{2-} ions can be replaced by the isoelectronic N^{3-} and F^- ions. They mainly indicated the structural equivalence of the nitride fluorides to the oxides in a majority of the cases. The alkaline earth compounds are unstable and are very sensitive to moisture.[13] A fundamental question of chemical ordering of N and F on the anion sublattice and its consequences to structure and electronic properties have not been addressed yet.

Structural information on the *stable* Zn_2NF available in the literature is elementary and does not provide the necessary details for understanding the electronic structure and properties.[18] We have examined the variation in band gap of ZnO with progressive substitution of N and F, especially the former because the upper most band in N,F-ZnO is primarily derived from N (2p) states while the F levels are deep down in energy.[7] The band gap variation of N-content in magnesium nitride fluorides reported in the literature is incomplete.[8] Here two-way feedback between experiment and detailed first-principles

Received: April 24, 2016
Published: June 14, 2016

DOI: 10.1021/jacs.6b04198
J. Am. Chem. Soc. 2016, 138, 8228−8234

calculations has been used to (a) ascertain the structure and (b) understand electronic properties of Zn_2NF and oxygen-doped Zn_2NF. The theoretical predictions are verified experimentally as illustrated by the visible-light-induced splitting of water to generate hydrogen. Furthermore, oxygen-doped Zn_2NF is p-type material and comes closest to the much-desired p-type ZnO. The results reported in this article would be of considerable value to those interested in using ZnO-based materials for hydrogen generation,[19−21] photovoltaics,[22,23] and other areas.[24]

2. METHODS

Zn_3N_2 precursor was prepared by the heating Zn metal powder in NH_3 at 500 °C. Zn_2NF was prepared by heating a pressed pellet of a 1:1 mol ratio of an intimate mixture of Zn_3N_2 (synthesized) and ZnF_2 (commercial). In a typical synthesis, the pellet was covered with a ceramic tube and sealed in a quartz ampule under vacuum (3×10^{-5} mbar). The sample was heated at 350 °C for 1 h and 500 °C for 2 h in a tube furnace. After the reaction was complete, the sample was collected from the quartz tube and subjected for characterization. Tetragonal Zn_2NF was obtained by heating the sample at above 500 °C. $ZnO_{0.2}N_{0.5}F_{0.3}$ was obtained by a similar procedure wherein the pellet was directly transferred to the quartz ampule and sealed. Photocatalytic hydrogen evolution studies were carried out by dispersing 20 mg of the photocatalyst in 75 mL of water containing 0.1 M Na_2S and 0.1 M Na_2SO_3. Samples were irradiated with a Xe lamp (Newport, 400 W), and hydrogen was detected and quantified with a gas chromatograph (PerkinElmer, Clarus 580).

We have carried out first-principles density functional theory (DFT)-based calculations using Quantum Espresso implementation,[25] with nonrelativistic Martins−Troullier norm-conserving pseudopotentials and exchange-correlation energy functional of Perdew−Wang (PW) within a local density approximation (LDA).[26] For Zn, O, N, and F, we included valence electrons in $3d^{10}4s^2$, $2s^22p^4$, $2s^22p^3$, and $2s^22p^5$ configurations, respectively. We simulated the wurtzite form of ZnO with space group $P6_3mc$ (no. 186) with two formula units in the primitive unit cell. Zn_2NF is experimentally found to crystallize in tetragonal as well as orthorhombic structures. In contrast, the samples of Zn_2NF with traces of oxygen crystallize in the hexagonal (wurtzite) structure similar to that of ZnO, with most anion sites being occupied by N and F. As there are many configurations of chemical ordering of N and F at O sites, we used the site occupancy disorder (SOD) technique[27] to determine the symmetry -inequivalent configurations in a $2 \times 2 \times 1$ supercell. This analysis provides insight into the specific configurations of N and F ordering on the anionic lattice that are energetically favorable and is relevant to tetragonal and orthorhombic structures as well. Plane wave basis sets used in the representation of wave functions and charge density were truncated at energy cut-offs of 80 and 320 Ry, respectively. A $6 \times 6 \times 5$ mesh of k points for tetragonal and orthorhomic systems and $6 \times 6 \times 8$ mesh of k points for a 16-atom ($2 \times 2 \times 1$) hexagonal supercell were used in sampling integrations over the Brillouin zone. Structural relaxation was performed for each system to minimize energy until the magnitude of Hellman−Feynman force on each atom was less than 0.01 eV/Å and the magnitude of stresses was within 1 kbar. We used these relaxed structures, in the determination and analysis of the electronic structure and its relevance to photocatalysis. As the electronic band gap is typically underestimated in DFT calculations, the Heyd−Scuseria−Ernzerhof (HSE-06) hybrid functional was used to obtain more accurate estimates of the band gap. We note that both HSE-based calculations and self-interaction corrected GW calculations[28] give similar estimates of the band gap of ZnO, which are 25% underestimated.

3. RESULTS AND DISCUSSION

Experimental Results on Zn_2NF and Other Compositions. We have prepared Zn_2NF by heating a pressed pellet of an intimate mixture of Zn_3N_2 and ZnF_2. Depending on the reaction temperature, we obtain Zn_2NF in tetragonal and orthorhombic crystal structures. In Figure 1, we show X-ray diffraction patterns of the two structures. The change in structure of Zn_2NF is clearly related to the ordering of the N^{3-} and F^- anions. Interestingly, $ZnO_{0.2}N_{0.5}F_{0.3}$ with the same nitrogen content occurs in the wurtzite structure of ZnO (Figure 1). The structure of Zn_2NF (tetragonal) was solved by Rietveld refinement of the powder XRD data (Supporting Information Figure S1). A systematic analysis of the data reveals that the (00l) and (0k0) reflections are systematically absent in the diffraction patterns. The (00l) and (0k0) reflections are only present at $l = 4n$ and $k = 2n$ (where n is an integer), respectively. Thus, $P4_12_12$ is the probable space group for Zn_2NF in the tetragonal structure. We have obtained the best fit of the diffraction data with a structure generated with a space group $P4_12_12$ (no. 92) with unit cell parameters a = 5.873 Å and c= 6.532 Å (Supporting Information Figure S1 and Table S2). In this structure, four formula units of Zn_2NF are present in the unit cell (Figure 2). The Zn atoms form distorted tetrahedra with two N and two F atoms. The N and F atoms form distorted tetrahedra with four Zn atoms. The Zn−N bond distances are 1.86 and 1.94 Å, and Zn−F bond distances are 2.05 and 2.56 Å. The Zn−N bond distances are smaller while the Zn−F bond distances are higher compared to the Zn−O bond distance (1.98 Å) in ZnO (Supporting Information Table S3). The deviation from the tetrahedral bonding and a large spread in bond distances in this structure arise from the existence of four-, six-, and eight-membered rings (Figure 2c). Four-membered rings consisting of two Zn, one N, and one F are of interest to examine whether they involve strained bonds. In the four-membered ring, Zn−N−Zn and N−Zn−F bond angles are 106.4° (tetrahedral) and 89.3° (square planar), respectively, causing a large increase in the Zn−F bond lengths and decrease in the Zn−F−Zn angle (Table S3). In the case of strain-free rings, the Zn−N bond distance slightly decreases and the Zn−F bond distance increases. These values of bond angles for the refined structure are in good agreement with the corresponding values from the theoretically predicted structure (Table S3). The structural feature of four-membered rings of Zn_2NF is similar to Zn_2O_2 and Ti_2O_2 dimers described

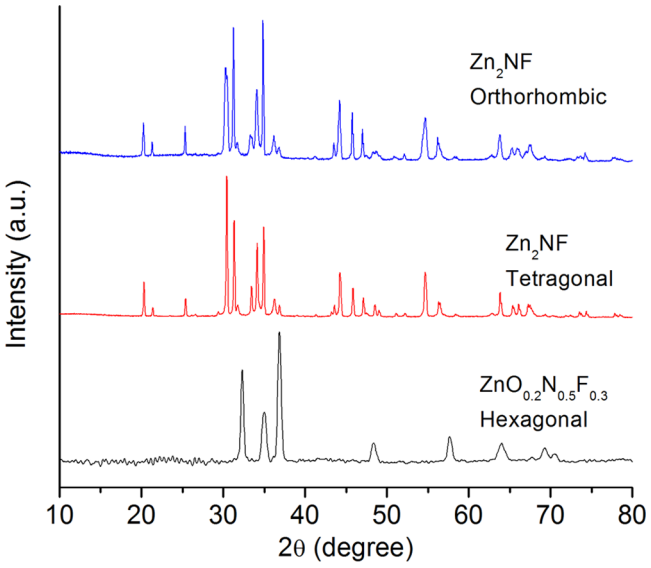

Figure 1. X-ray diffraction patterns of tetragonal Zn_2NF, orthorhombic Zn_2NF, and $ZnO_{0.2}N_{0.5}F_{0.3}$ (wurtzite structure).

DOI: 10.1021/jacs.6b04198
J. Am. Chem. Soc. 2016, 138, 8228−8234

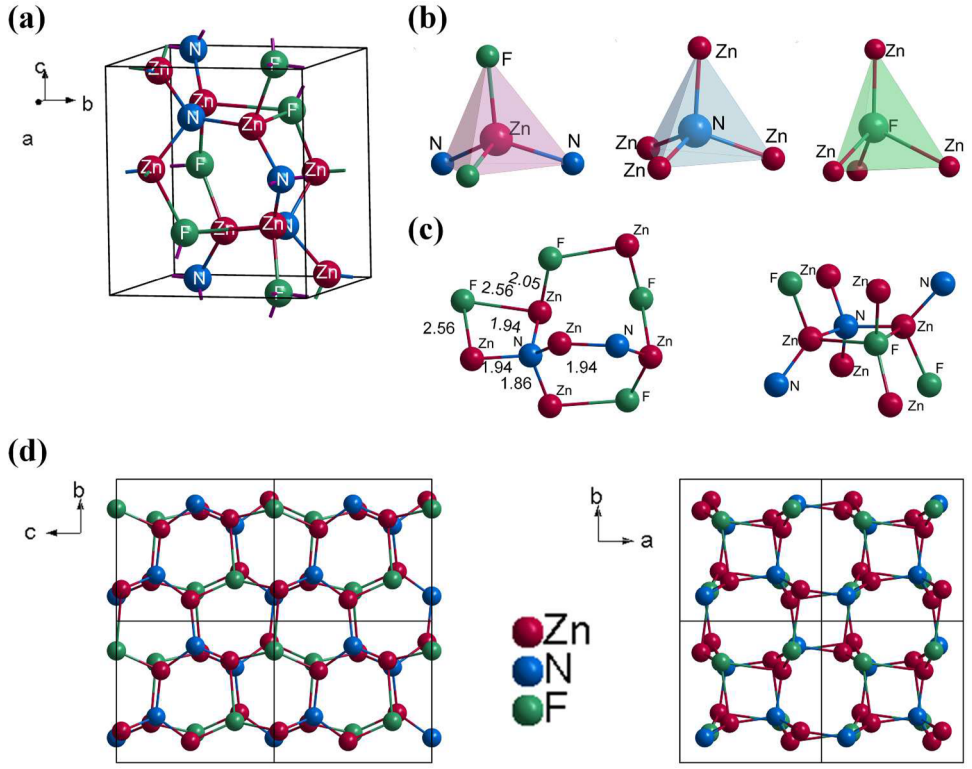

Figure 2. Representation of (a) atomic arrangement in the unit cell, (b) tetrahedral coordination at Zn, N, and F, (c) four-, six-, and eight-membered rings, and (d) projection of 2 × 2 × 2 supercell structures along *a* and *c* axis directions of tetragonal Zn_2NF. (The bond lengths are given in Å units).

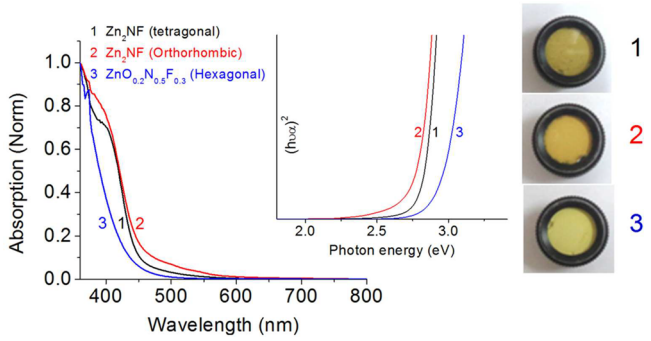

Figure 3. Electronic absorption spectra of tetragonal Zn_2NF, orthorhombic Zn_2NF, and $ZnO_{0.2}N_{0.5}F_{0.3}$. Inset shows the corresponding tauc plot. Colors of the samples are indicated in photographs.

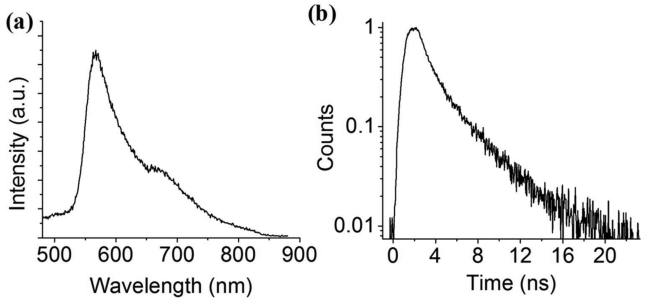

Figure 4. (a) Photoluminescence and (b) decay kinetics of orthorhombic Zn_2NF.

previously.[29,30] Tetragonal Zn_2NF is isostructural to γ-$LiAlO_2$ wherein the N atoms replace Al, F replaces Li, and Zn replaces O.[31] The orthorhombic structure would be derived from the nonisomorphic subspace group of $P4_12_12$ ($P2_12_12_1$, no. 19) (Supporting Information Figure S2, Table S4). The unit cell parameters to be a = 5.850 Å, b = 5.892 Å, and c = 6.536 Å. The coordination geometry of Zn, N, and F in this structure is similar to that of the tetragonal structure with a slight variation in the bond lengths and angles (Figure S3).

In Figure 3, we show the optical absorption spectra of Zn_2NF in the tetragonal and orthorhombic structures. Both samples show typical semiconductor absorption spectra with extended visible absorption. The tauc plots given as the inset in the figure reveal a linear relationship of $(h\nu\alpha)^{1/n}$ vs $h\nu$ where n = 1/2, indicating the direct band gap. The estimated band gaps of Zn_2NF in the tetragonal and orthorhombic structures are 2.8 and 2.7 eV, respectively. The band edge of Zn_2NF is significantly red-shifted compared to that of ZnO (3.2 eV). The band edges are only slightly different from that of $ZnO_{0.2}N_{0.5}F_{0.3}$ (2.8 eV) which has the same N content. Zn_2NF samples are yellow colored (Figure 3).

The photoluminescence spectrum of orthorhombic Zn_2NF at room temperature is shown in Figure 4a. Upon excitation at 450 nm, Zn_2NF gives emission bands centered at 565 and 670 nm. To determine the nature of luminescence, we have collected decay kinetics of these materials (Figure 4b). We see that the major component in the decay channels has a lifetime of ∼1 ns and a minor component with a lifetime 3−4 ns.

We have examined the variation in band gap of $ZnO_{1-x-y}N_xF_y$ by preparing a few compositions of N,F-doped ZnO. The nitrogen content in these materials is more crucial because the N (2p) states occupy the top of the valence band and determine the band gap, the F^- states lying deep down in energy and do not affect the band gap.[7] In Figure 5, we show a plot of the band gap against the nitrogen content. The band gap of ZnO decreases initially on incorporation of N^{3-} up to a

DOI: 10.1021/jacs.6b04198
J. Am. Chem. Soc. 2016, 138, 8228−8234

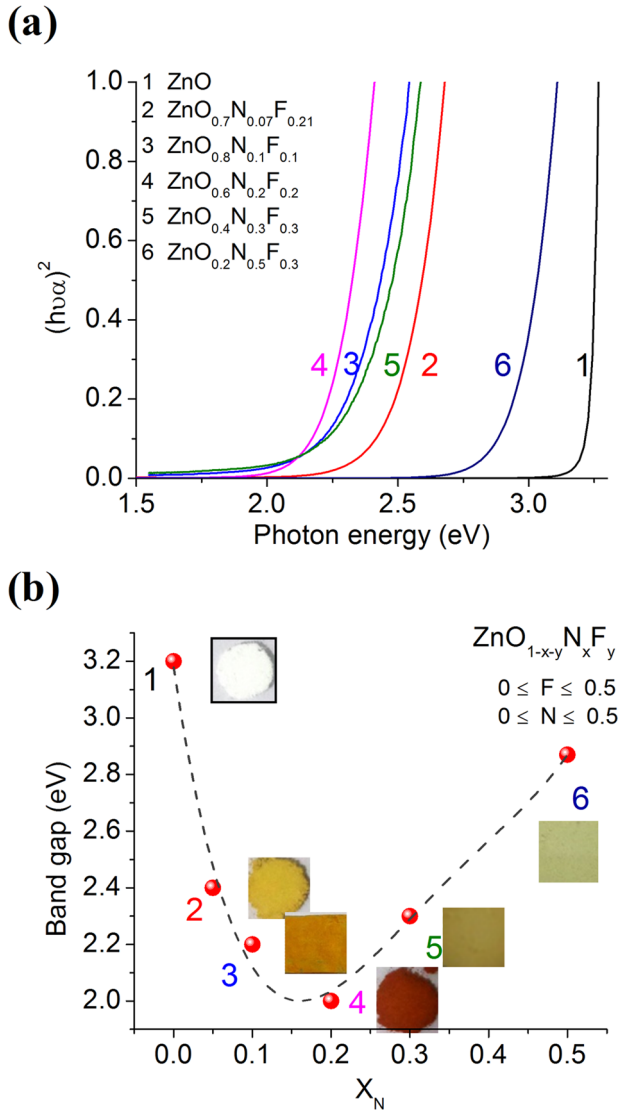

Figure 5. (a) Tauc plots of ZnO doped with different amounts of N and F and (b) variation of band gap with the amount of N in N- and F-doped ZnO. Colors of the samples are indicated in photographs.

Table 1. Comparison of Lattice Parameters Obtained Using LDA Norm-Conserving Pseudopotentials with the Experimental Values

system	lattice constant (Å)	
	experimental	LDA-NC
ZnO	a = 3.25	a = 3.20
	c = 5.21	c = 5.15
Zn_2NF (tetragonal)	a = 5.87	a = 5.73
	c = 6.53	b = 5.76
		c = 6.40
Zn_2NF (orthorhombic)	a = 5.85	a = 5.72
	b = 5.89	b = 5.77
	c = 6.54	c = 6.40

concentration above which the band gap increases. This is expected because the values of the band gap of tetragonal and orthorhombic Zn_2NF are 2.8 and 2.7 eV, respectively, while that of $ZnO_{0.2}N_{0.5}F_{0.3}$ is 2.8 eV. In a recent report, the band gap in magnesium-nitride-fluorides that decreases with the increase

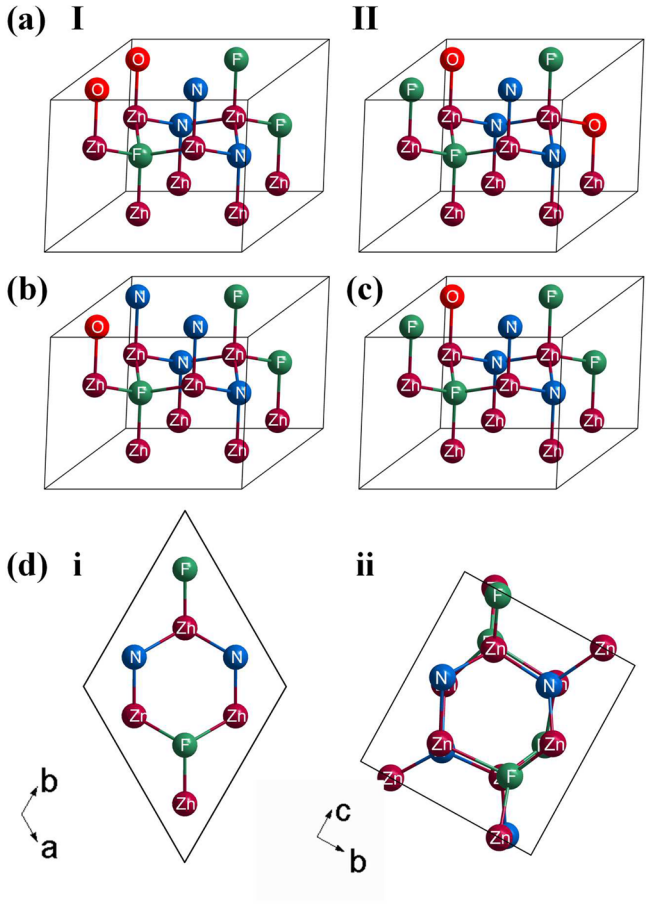

Figure 6. Crystal structure and anionic ordering of (a) $Zn_8O_2N_3F_3$ (hexagonal) configurations I and II, (b) $Zn_8ON_4F_3$ (hexagonal), and (c) $Zn_8ON_3F_4$ (hexagonal). (d) Comparison of crystal structures of Zn_2NF: (i) hexagonal (configuration-4), (ii) tetragonal (orthorhombic structure is weakly distorted from the tetragonal structure) [color code: maroon, Zn; red, O; blue, N; green, F].

Table 2. Comparison of Band Gaps Estimated from Calculations Based on LDA and HSE Functional with Those from Experiment

system	band gap (eV)		
	LDA-NC	HSE	experimental
ZnO	0.69	2.34	3.3
Zn_2NF (hexagonal, C-4))	0.53	1.96	-
$Zn_8O_2N_3F_3$ (hexagonal, C-I)	0.18	1.57	2.8
$Zn_8O_2N_3F_3$ (hexagonal, C-II)	0.12	1.52	
Zn_2NF (tetragonal)	1.31	2.76	2.8
Zn_2NF (orthorhombic)	1.31	2.76	2.7

in nitrogen content is only partially correct and applies only up to a particular nitrogen content.[8]

The diffuse-reflectance spectra of $ZnO_{0.2}N_{0.5}F_{0.3}$ and $ZnO_{0.7}N_{0.07}F_{0.21}$ show a characteristic band in the near IR region in addition to the band-to-band transition in the visible region (Figure S4), somewhat similar to conducting oxide films.[32] We assign this new band as the response of the excess-charge carriers present in the system because of the unequal incorporation of N and F.

Results of First-Principles Calculations. Our estimates of the lattice constants obtained for ZnO and Zn_2NF from first-principles calculations agree with experiment within the typical

DOI: 10.1021/jacs.6b04198
J. Am. Chem. Soc. 2016, 138, 8228−8234

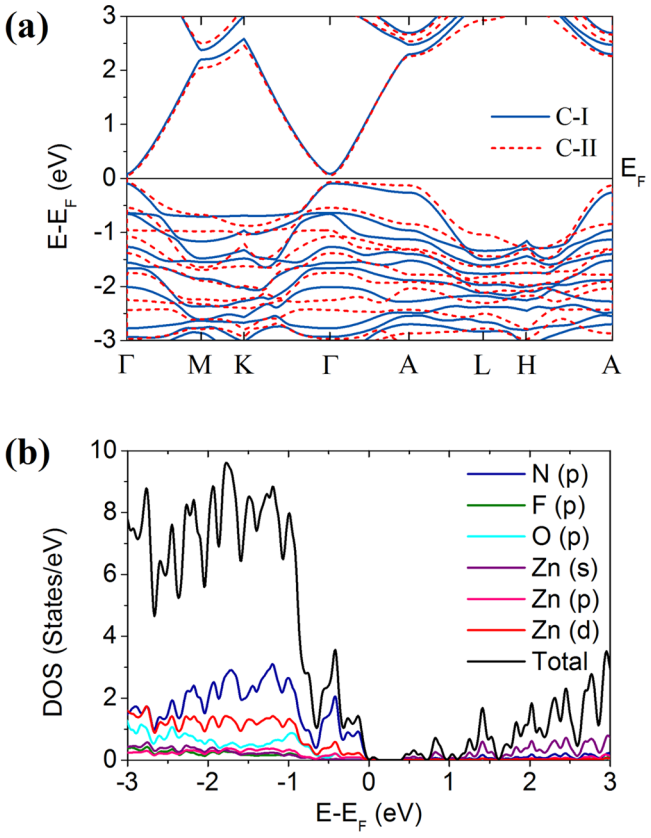

Figure 7. (a) Electronic structure of $Zn_8O_2N_3F_3$ (hexagonal) [blue solid line, configuration I; red broken line, configuration II] and (b) density of electronic states of $Zn_8O_2N_3F_3$ (hexagonal) (configuration II) [Fermi energy is set at 0 eV].

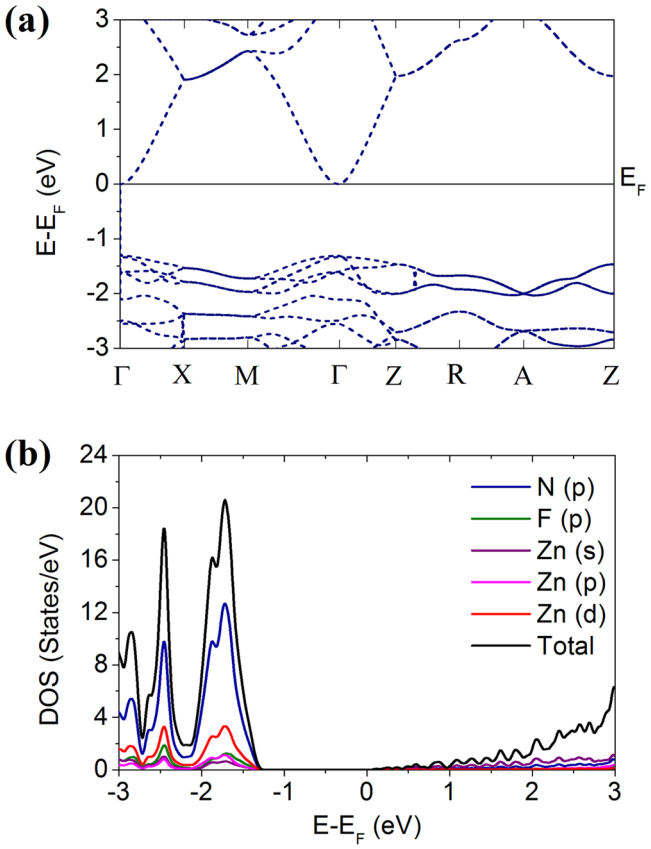

Figure 8. (a) Electronic structure and (b) density of electronic states of Zn_2NF (orthorhombic) [Fermi energy is set at 0 eV].

DFT errors (Table 1). In ZnO, underestimation of the band gap occurs partly due to relatively strong coupling between p-states of oxygen and the fully occupied d-states of Zn, bands of which are close in energy (Supporting Information Figure S5a).[33] The valence band in ZnO is constituted primarily of O 2p orbitals and lower energy band of 3d orbitals of Zn, while the conduction bands have a predominant character of 4s orbitals of Zn (Figure S5b).

We first considered Zn_2NF in the hexagonal structure and chemical ordering of N and F to understand the electronic structure of $ZnO_{0.2}N_{0.5}F_{0.3}$ in the wurtzite structure (Figure 6). We find that the in-plane "*a*" lattice parameter is essentially unchanged upon N, F substitution, while the value of the "*c*" parameter increases by 1.36% for Zn_2NF in the wurtzite structure. In the 2 × 2 × 1 supercell of Zn_2NF, there are 72 configurations corresponding to the occupation of 4 N and 4 F at the 8 O sites. The SOD technique (see Methods) reduces them to 12 symmetry inequivalent configurations (Supporting Information Figure S6). We have calculated electronic structures of all the 12 configurations and find that 10 of them exhibit metallic electronic structure and 2 of them (configurations 4 and 11) are semiconducting with a nonzero gap. These are also the lowest energy states. The electronic structure of Zn_2NF with the lowest energy (configuration 4) is interesting (Supporting Information Figure S7a). While the top of its valence band is constituted mainly of N 2p orbitals, its conduction band retains the Zn 4s orbital character. Contribution of Zn 3d states is more prominent to states ∼1.5 eV below the valence band maximum (Figure S7b). The band gap obtained with HSE-06 functional (Table 2) for Zn_2NF (hexagonal) is about 0.4 eV less than that of ZnO. In simulations of the samples containing oxygen, we used the same supercell for the compositions $Zn_8O_2N_3F_3$ (with two inequivalent configurations), $Zn_8ON_3F_4$, and $Zn_8ON_4F_3$ (Figure 6). For $Zn_8O_2N_3F_3$, configuration II is more stable than configuration I by ∼16 meV per supercell. The presence of oxygen further decreases the band gap of Zn_2NF to 1.52 eV in $Zn_8O_2N_3F_3$ (Figure 7a, Table 2). Here we see that the top of the valence band is constituted mainly of N 2p and weakly of Zn 3d orbitals mixed with O 2p orbitals, while the conduction band retains its Zn 4s character (Figure 7b). The electronic structure of $Zn_8ON_4F_3$ exhibits p-type character with the Fermi level within the valence band (near the top), while $Zn_8ON_3F_4$ exhibits n-type character with Fermi level within the conduction band (near the bottom) (Supporting Information Figure S8).

Anionic ordering in tetragonal Zn_2NF was derived from the one in the hexagonal structure (Figure 6). The structure, upon full relaxation with respect to lattice parameters and the atomic positions, becomes weakly an orthorhombic (Table 1), which is ∼1.02 eV more stable than its hypothetical hexagonal wurtzite structure. The tetragonal form of Zn_2NF has the space group of $P4_12_12$ (no. 92) with tetrahedral coordination which is the γ-$LiAlO_2$ structure. This structure is closely related to the wurtzite structure and can be obtained by straining the latter (Figure 6). From the electronic structure (shown in Figure 8a), it is clear that the top of the valence band is constituted mainly of N 2p orbitals and weakly of Zn 3d orbitals (Figure 8b). The conduction band retains the Zn 4s character, similar to Zn_2NF

DOI: 10.1021/jacs.6b04198
J. Am. Chem. Soc. 2016, 138, 8228−8234

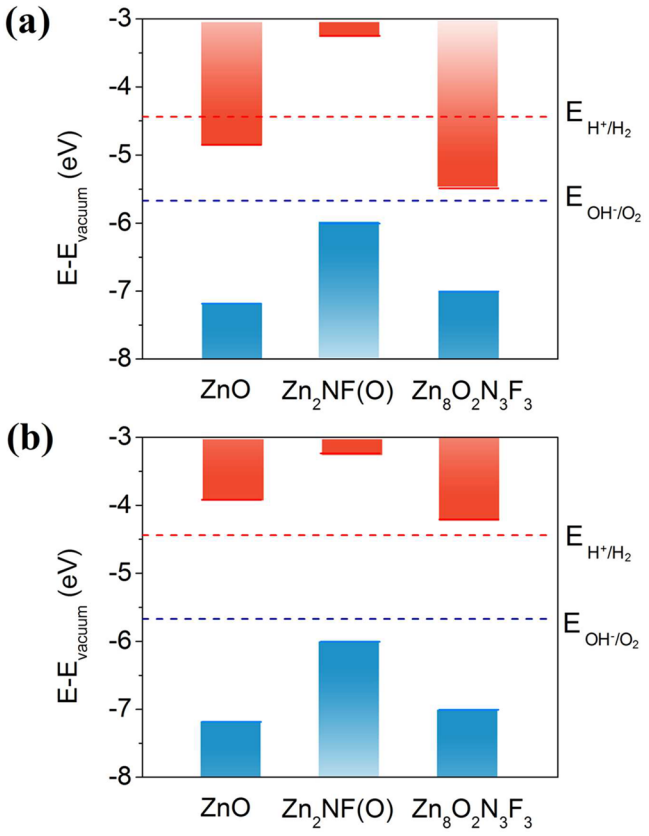

Figure 9. Alignment of valence and conduction bands of ZnO, Zn_2NF (O), and $Zn_8O_2N_3F_3$ obtained using (a) calculations based on HSE functional and (b) experimental band gaps to position the conduction bands.

with the hypothetical hexagonal structure considered previously. Our estimate of the band gap of Zn_2NF obtained with the HSE-06 functional is 2.76 eV, which is in good agreement with the experimental value.

To determine the suitability of $ZnO_xN_yF_z$ for use in photocatalytic water splitting, we have aligned their valence and conduction band edges with respect to vacuum and compared with the redox potentials relevant to water-splitting reactions (Figure 9). Though calculations with the HSE functional give better estimates of the band gap than with LDA, the improvement is not quite complete in some of the cases, particularly in ZnO and related materials. Hence, we use the scissor correction by taking the experimental band gaps as input in alignment of the conduction bands. We find that the valence band maxima and the conduction band minima straddle the redox potentials of hydrogen evolution reaction (HER) and oxygen evolution reaction (OER). Thus, both Zn_2NF (orthorhombic) and Zn_2NF with O content (hexagonal) are expected to be good photocatalysts for water splitting.

Hydrogen Evolution from Water Splitting. Developing a novel semiconductor with visible-light-induced photocatalytic activity has been in demand in recent years.[34] Because zinc nitride fluorides absorb visible-light and possess suitable band positions for photocatalytic water splitting, we have tested them for the production of hydrogen from water. Photocatalytic hydrogen evolution studies on orthorhombic Zn_2NF and $ZnO_{0.2}N_{0.5}F_{0.3}$ were carried out in the presence of 0.1 M Na_2S and 0.1 M Na_2SO_3 as sacrificial agents under visible-light irradiation. In Figure 10a, we present the photocatalytic hydrogen evolution data on these materials having deposited Pt. Both these materials exhibit hydrogen evolution activity under visible light irradiation. However, orthorhombic Zn_2NF/Pt exhibits higher hydrogen evolution activity (220 μmol h^{-1} g^{-1}) compared to $ZnO_{0.2}N_{0.5}F_{0.3}$/Pt (114 μmol h^{-1} g^{-1}). We have also examined the photocatalytic activity of Zn_2NF without Pt and find remarkable hydrogen evolution activity even in the absence of Pt. In Figure 10b, we compare the activity of orthorhombic Zn_2NF with and without Pt. Nearly 30% of the activity (68 μmol h^{-1} g^{-1}) is retained in the absence of Pt. Tetragonal Zn_2NF also shows photocatalytic activity in the presence or absence of Pt, although the activity is somewhat smaller (Supporting Information Figure S9). To see the long-term stability and recyclability of the photocatalyst, we have carried out cyclic test with orthorhombic Zn_2NF/Pt (Supporting Information Figure S10) and find that the activity of the material is enhanced in a period 2 h and retained the same activity (402 μmol h^{-1} g^{-1}) in further cycles. It is to be noted that the ZnO has no activity for hydrogen evolution under visible-light irradiation.

4. CONCLUSIONS

It has been possible to synthesize and characterize Zn_2NF which is the ultimate composition resulting from substitution of O^{2-} in ZnO by aliovalent N^{3-} and F^- anions. This material exhibits remarkable properties with visible absorption and a significantly reduced band gap (2.75 eV). It is interesting that

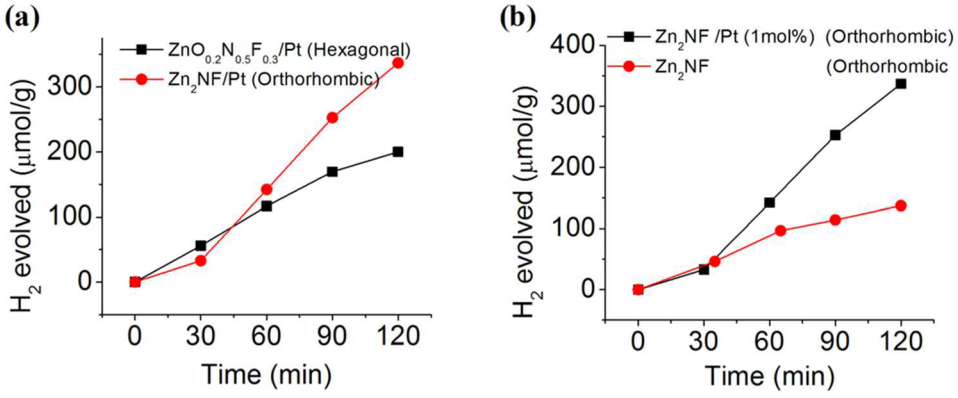

Figure 10. Comparison of photocatalytic hydrogen evolution: (a) $ZnO_{0.2}N_{0.5}F_{0.3}$/Pt and orthorhombic Zn_2NF/Pt; (b) orthorhombic Zn_2NF/Pt and orthorhombic Zn_2NF.

DOI: 10.1021/jacs.6b04198
J. Am. Chem. Soc. 2016, 138, 8228−8234

while Zn_2NF is tetragonal or orthorhombic, $ZnO_{0.2}N_{0.5}F_{0.3}$ retains the wurtzite structure of ZnO, with a smaller band gap. First-principles calculations throw light on the electronic structure of Zn_2NF and related materials. The tetragonal and orthorhombic structures of Zn_2NF found experimentally are more stable than the hexagonal structure. First-principles calculations indicate $ZnO_{0.2}N_{0.5}F_{0.3}$ to be a p-type semiconductor. It appears that this material is probably closest to the elusive p-type ZnO. Furthermore, the CB and VB edges of Zn_2NF are favorably placed for water splitting as indeed found experimentally. The present study is a fine example of band tuning by aliovalent anion substitution, wherein the p-orbitals of the substituent anions plays a crucial role.

■ ASSOCIATED CONTENT

Supporting Information

The Supporting Information is available free of charge on the ACS Publications website at DOI: 10.1021/jacs.6b04198.

Materials synthesis, characterization techniques, photocatalytic hydrogen evolution, XRD patterns of N- and F-doped ZnO, XPS spectra of N- and F-doped ZnO, electronic structure of ZnO, Zn_2NF (hexagonal), $Zn_8ON_4F_3$, and $Zn_8ON_3F_4$ (PDF)

■ AUTHOR INFORMATION

Corresponding Author

*cnrrao@jncasr.ac.in

Author Contributions

The manuscript was written through contributions of all authors. All authors have given approval to the final version of the manuscript.

Notes

The authors declare no competing financial interest.

■ ACKNOWLEDGMENTS

S.R.L. is grateful to Council of Scientific and Industrial Research, India, for the SRF fellowship. S.R.L. and K.M. are grateful to Sheikh Saqr Laboratory for the fellowship. U.S.S. and U.V.W. thank the Department of Science and Technology, government of India for support through TUE-CMS and a JC Bose National Fellowship, respectively.

■ REFERENCES

(1) Stavrinadis, A.; Rath, A. K.; de Arquer, F. P. G.; Diedenhofen, S. L.; Magén, C.; Martinez, L.; So, D.; Konstantatos, G. *Nat. Commun.* **2013**, *4*, 2981.

(2) Fujito, H.; Kunioku, H.; Kato, D.; Suzuki, H.; Higashi, M.; Kageyama, H.; Abe, R. *J. Am. Chem. Soc.* **2016**, *138*, 2082−2085.

(3) Phillips, J. C. *Bonds and bands in semiconductors*; Academic Press, New York: 1973.

(4) Maeda, K.; Domen, K. *J. Phys. Chem. C* **2007**, *111*, 7851−7861.

(5) Li, C.; Wei, J.; Sato, M.; Koike, H.; Xie, Z.-Z.; Li, Y.-Q.; Kanai, K.; Kera, S.; Ueno, N.; Tang, J.-X. *ACS Appl. Mater. Interfaces* **2016**, *8*, 11526−11531.

(6) Jansen, M.; Letschert, H. P. *Nature* **2000**, *404*, 980−982.

(7) Rao, C. N. R. *J. Phys. Chem. Lett.* **2015**, *6*, 3303−3308.

(8) Fang, C. M.; Ramanujachary, K. V.; Hintzen, H. T.; de With, G. *J. Alloys Compd.* **2003**, *351*, 72−76.

(9) Saha, R.; Revoju, S.; Hegde, V. I.; Waghmare, U. V.; Sundaresan, A.; Rao, C. N. R. *ChemPhysChem* **2013**, *14*, 2672−2677.

(10) Lingampalli, S. R.; Rao, C. N. R. *J. Mater. Chem. A* **2014**, *2*, 7702−7705.

(11) Shen, G.; Cho, J. H.; Yoo, J. K.; Yi, G.-C.; Lee, C. J. *J. Phys. Chem. B* **2005**, *109*, 5491−5496.

(12) Stavale, F.; Pascua, L.; Nilius, N.; Freund, H.-J. *J. Phys. Chem. C* **2014**, *118*, 13693−13696.

(13) Ehrlich, P.; Linz, W.; Seifert, H. J. *Naturwissenschaften* **1971**, *58*, 219−220.

(14) Zhu, L.; Chen, X.; Yamanaka, S. *Solid State Commun.* **2004**, *130*, 227−230.

(15) Wüstefeld, C.; Vogt, T.; Löchner, U.; Strähle, J.; Fuess, H. *Angew. Chem.* **1988**, *100*, 1013−1013.

(16) Andersson, S. *Ark. Kemi* **1967**, *26*, 521.

(17) Andersson, S. *J. Solid State Chem.* **1970**, *1*, 306−309.

(18) Marchand, R.; Lang, J. *Mater. Res. Bull.* **1971**, *6*, 845−852.

(19) Chen, H. M.; Chen, C. K.; Chang, Y.-C.; Tsai, C.-W.; Liu, R.-S.; Hu, S.-F.; Chang, W.-S.; Chen, K.-H. *Angew. Chem., Int. Ed.* **2010**, *49*, 5966−5969.

(20) Lingampalli, S. R.; Gautam, U. K.; Rao, C. N. R. *Energy Environ. Sci.* **2013**, *6*, 3589−3594.

(21) Zhong, M.; Ma, Y.; Oleynikov, P.; Domen, K.; Delaunay, J.-J. *Energy Environ. Sci.* **2014**, *7*, 1693−1699.

(22) Anta, J. A.; Guillén, E.; Tena-Zaera, R. *J. Phys. Chem. C* **2012**, *116*, 11413−11425.

(23) Zhang, Q.; Dandeneau, C. S.; Zhou, X.; Cao, G. *Adv. Mater.* **2009**, *21*, 4087−4108.

(24) Wang, Z. L. *J. Phys.: Condens. Matter* **2004**, *16*, R829.

(25) Giannozzi, P.; Baroni, S.; Bonini, N.; Calandra, M.; Car, R.; Cavazzoni, C.; Ceresoli, D.; Chiarotti, G. L.; Cococcioni, M.; Dabo, I.; Corso, A. D.; Gironcoli, S. d.; Fabris, S.; Fratesi, G.; Gebauer, R.; Gerstmann, U.; Gougoussis, C.; Kokalj, A.; Lazzeri, M.; Martin-Samos, L.; Marzari, N.; Mauri, F.; Mazzarello, R.; Paolini, S.; Pasquarello, A.; Paulatto, L.; Sbraccia, C.; Scandolo, S.; Sclauzero, G.; Seitsonen, A. P.; Smogunov, A.; Umari, P.; Wentzcovitch, R. M. *J. Phys.: Condens. Matter* **2009**, *21*, 395502.

(26) Perdew, J. P.; Wang, Y. *Phys. Rev. B: Condens. Matter Mater. Phys.* **1992**, *45*, 13244−13249.

(27) Grau-Crespo, R.; Hamad, S.; Catlow, C. R. A.; Leeuw, N. H. d. *J. Phys.: Condens. Matter* **2007**, *19*, 256201.

(28) Usuda, M.; Hamada, N.; Kotani, T.; van Schilfgaarde, M. *Phys. Rev. B: Condens. Matter Mater. Phys.* **2002**, *66*, 125101.

(29) Neeraj, S.; Natarajan, S.; Rao, C. N. R. *New J. Chem.* **1999**, *23*, 303−307.

(30) Anantharaman, G.; Roesky, H. W.; Schmidt, H.-G.; Noltemeyer, M.; Pinkas, J. *Inorg. Chem.* **2003**, *42*, 970−973.

(31) Marezio, M. *Acta Crystallogr.* **1965**, *19*, 396−400.

(32) Vai, A. T.; Kuznetsov, V. L.; Jain, H.; Slocombe, D.; Rashidi, N.; Pepper, M.; Edwards, P. P. *Z. Anorg. Allg. Chem.* **2014**, *640*, 1054−1062.

(33) Schröer, P.; Krüger, P.; Pollmann, J. *Phys. Rev. B: Condens. Matter Mater. Phys.* **1993**, *47*, 6971−6980.

(34) Kamat, P. V.; Bisquert, J. *J. Phys. Chem. C* **2013**, *117*, 14873−14875.

DOI: 10.1021/jacs.6b04198
J. Am. Chem. Soc. 2016, 138, 8228−8234